



Impact of Silicone Oil on Free Fatty Acid Particle Formation due to Polysorbate 20 Degradation

Raphael Fish¹ · Jasper Lin² · Nidhi Doshi²

Received: 9 July 2020 / Accepted: 22 September 2020 / Published online: 7 October 2020
© Springer Science+Business Media, LLC, part of Springer Nature 2020

ABSTRACT

Purpose Polysorbate 20 (PS20), a commonly used surfactant in biopharmaceutical formulations, can undergo hydrolytic degradation resulting in free fatty acids (FFAs) that precipitate to form particles. This work investigates the ability for silicone oil (si-oil) coated on the interior walls of prefilled syringes (PFSs) to act as a sink for FFAs and potentially delay FFA particle formation.

Methods Myristic acid distribution coefficient was measured in a two-phase system containing si-oil and formulation buffer at a range of aqueous conditions. An empirical model was built from these data to predict distribution coefficient based on aqueous conditions. To verify the model, PS20 was degraded using model lipases side-by-side in glass vials and PFSs while monitoring sub-visible particles.

Results The empirical model demonstrates that the partitioning of myristic acid into si-oil is maximized at low pH and low PS20 concentration. The model predicts that the presence of si-oil at levels typical in PFSs provides at most an 8.5% increase in the total carrying capacity for myristic acid compared to a non-coated glass vial. The time to onset of FFA particles was equivalent between degradations performed in two PFS models coated with differing levels of silicone oil and in non-coated glass vials.

Conclusion Herein, we demonstrate that FFAs partition from aqueous solution into si-oil. However, the extent of the partitioning effect is not large enough to delay PS20-related FFA particle formation at typical formulation conditions (pH 5.0–

7.5, 0.01% - 0.1% w/v PS20) filled in typical PFSs (<1.0 mg si-oil/mL aqueous fill).

KEY WORDS formulation · free fatty acid · particles · polysorbate degradation · silicone oil

ABBREVIATIONS

FFA	Free fatty acid
PFS	Pre-filled syringe
PS20	Polysorbate-20
SI-OIL	Silicone oil
FB	Formulation buffer
D	Distribution coefficient
P	Partition coefficient
PCL	Pseudomonas cepacea lipase
CALB	Candida antarctica lipase B
RP-UHPLC	Reverse-phase ultra-high performance liquid chromatography
MM-HPLC	Mixed-mode high performance liquid chromatography
ELSD	Evaporative light scattering detection
RP-HPLC	Reverse-phase high performance liquid chromatography
HA	Protonated (non-ionized) fatty acid
A ⁻	Deprotonated (ionized) fatty acid

INTRODUCTION

Polysorbate 20 (PS20) is a heterogeneous non-ionic surfactant commonly used in the formulation of biopharmaceutical drug products (DPs) to protect protein from interfacial stresses (1–4). PS20 consists of a mixture of closely related compounds, comprised of a sorbitan head group with a fatty acid side chain

✉ Nidhi Doshi
doshin1@gene.com

¹ Purification Development, Genentech Inc., 1 DNA Way, South San Francisco, California 94080, USA

² Pharmaceutical Development, Genentech Inc., 1 DNA Way, South San Francisco, California 94080, USA

of varying length, linked via an ester bond (5). Several publications have shown that PS20 can degrade during DP storage with substantial implications to long-term protein stability (6–10). PS20 has been shown to degrade hydrolytically at the ester bond linking the fatty acid side chain to the sorbitan head group via chemical or enzymatic mechanisms (11). Enzymes (lipases, esterases etc.) endogenous to the host cells used in the manufacture of therapeutic proteins can co-purify with the target protein and be present at trace levels in final formulated DPs. It is suspected that these trace enzymes hydrolyze the PS20 ester bond and are the root cause of PS20 degradation for several biopharmaceutical DPs (12).

Hydrolytic degradation of PS20 carries concern to long-term DP stability primarily because of the free fatty acid (FFA) byproducts of such degradation. FFAs have limited solubility in aqueous solution (13). Over time, the accumulation of FFAs resulting from hydrolytic PS20 degradation can result in precipitation, leading to the formation of visible and/or sub-visible particles (14). Particle formation in susceptible DPs poses a risk to product quality and, potentially, to patient safety. Recent publications have shown that numerous biopharmaceutical DPs formulated with PS20 are susceptible to this risk, with FFA particles appearing in some products after as little as 18 months of real time storage (8,9). Despite this risk, however, PS20 continues to be a common formulation excipient due to its many favorable properties as a surfactant.

There are several potential approaches to mitigate the risks associated with hydrolytic degradation of PS20. Recent mitigation efforts have ranged from engineering of host cell lines to reduce or eliminate lipase expression to exploration of alternative surfactants (15,16). A yet untested approach may involve modifying the design of the vessels used to store DP. Liquid biopharmaceutical DPs are traditionally filled into glass vials. In such presentation, DP is typically drawn into a syringe immediately before administration. However, pre-filled syringes (PFSs) are becoming increasingly prevalent due to increased convenience (17). In such a presentation, the DP is filled into syringes during the manufacturing process. This eliminates the need for the transfer of DP from vial to syringe prior to administration, simplifying the use of the product at point of use.

Moreover, the use of PFSs may offer some tangential benefit in the context of the aforementioned risk of PS20-related FFA particle formation. The interior walls of PFSs are typically coated with a thin layer of silicone oil (si-oil) (18). Si-oil acts as a lubricant during syringe use, allowing the stopper to glide smoothly down the barrel of the syringe when the plunger rod is depressed (18). The presence of si-oil in PFSs may also serve the unintended benefit of mitigating FFA particle formation risk. Si-oil is an inherently hydrophobic material that is near immiscible with water. In PFS systems filled with

aqueous biopharmaceutical formulations, the si-oil coatings essentially act as a distinct second phase.

Since the si-oil in PFSs is in direct contact with the aqueous liquid DP, solutes in the two-phase system should be subject to partitioning behavior. Hydrophilic compounds present in DP PFSs will theoretically favor the aqueous phase while hydrophobic compounds should partition largely into the oil phase. Given the relatively long time frames over which FFA particle formation has been observed in susceptible DPs (≥ 18 months as previously mentioned), partitioning behavior likely approaches dynamic equilibrium. On this principle, the highly immiscible FFAs released upon hydrolytic degradation of PS20 may partition from the aqueous phase where they are generated into the si-oil phase. If the extent of this partitioning effect is large enough, the use of siliconized PFSs may prevent or delay FFA particle formation relative to non-coated glass vials.

To investigate this hypothesis, the equilibrium partitioning behavior of FFA between si-oil and an aqueous buffer mimicking a biopharmaceutical liquid formulation was explored. The impact of formulation parameters on the partitioning behavior was characterized to provide an understanding of the levers available to modulate the extent of the partitioning effect. The results of the characterization were applied to the specific use case of DP in PFSs to determine the extent to which si-oil present in PFSs can help to mitigate the risk of FFA particle formation.

MATERIALS AND METHODS

Materials

TweenTM 20 HP (high purity) polysorbate 20 (PS20) was obtained from Croda (Edison, NJ). Dimethicone (si-oil) was obtained from Sigma-Aldrich (St. Louis, MO). L-histidine and histidine-HCl were obtained from Ajinomoto (Raleigh, NC). Sucrose was obtained from Pfanstiehl (Waukegan, IL). The enzymes *Candida antarctica lipase B* (CALB) and *Pseudomonas cepacea lipase* (PCL) were obtained in lyophilized form from Sigma-Aldrich (St. Louis, MO). Water used to prepare all solutions in this study was purified using an Elga PureLab Ultra filtration system (High Wycombe, United Kingdom).

A recombinant protein therapeutic, henceforth referred to as molecule-A, was obtained from Genentech (South San Francisco, CA). Studies were performed in formulation buffer (FB) composed of L-histidine, histidine hydrochloride and sucrose at low ionic strength (< 10 mM); henceforth referred to as FB-A. FB-A was made at pH values ranging from 5.0 to 7.5 and with PS20 concentrations ranging from 0.01 to 0.1% (w/v), based on the experimental conditions of interest. Additional properties of molecule-A such as hydrophobicity and molecular weight are confidential and cannot be disclosed.

However, we believe this does not affect the overall conclusions of the paper for reasons mentioned in the discussion section.

Two models of glass PFS were obtained. PFSs representative of the device used for molecule-A, henceforth referred to as PFS-A, were obtained from Genentech (South San Francisco, CA). The average ratio of si-oil mass to nominal fill volume is 0.026 mg/mL for PFS-A. The volume and si-oil mass/barrel for PFS-A are confidential and cannot be disclosed. Commercially available PFSs with a nominal volume of 2.25 mL and an average si-oil coating of 0.7 mg/barrel, henceforth referred to as PFS-B, were obtained from Becton-Dickinson (Franklin Lakes, NJ). PFS-B was considered a best-case PFS for FFA partitioning relative to the representative PFS-A, due to its relatively high level of si-oil. Uncoated glass vials with a nominal volume of 2 mL were obtained from Schott (Elmsford, NY). Rubber stoppers used for all sample vessels were free of si-oil coating.

Study Design

Part I: Free Fatty Acid Distribution Coefficient Model

Partitioning of Free Fatty Acid in a Two Phase System. The two-phase distribution coefficient of FFA was determined experimentally for myristic acid as summarized in Fig. 1. The solubility of myristic acid in FB-A was approximated for each tested condition using the semi-empirical model developed by Doshi, *et al.* (13). Myristic acid was dissolved in FB-A to approximately 60–80% of the calculated solubility limit using FFA dissolution methods previously described by Doshi *et al.* (13). Si-oil was overlaid gravimetrically on the FFA-in-FB-A system. The two-phase mixture was gently stirred overnight to equilibrate the distribution of myristic acid between the two phases in the system. Mixing was performed with glass magnetic stir-bars rather than Teflon coated magnetic stir bars to prevent potential surface adsorption of the hydrophobic analyte. Stirring speed was maintained below 200 rpm to minimize shear and prevent the nucleation of FFA particles. Experiments were performed at 5°C to mimic typical long-term aqueous DP storage conditions.

Calculation of Free Fatty Acid Distribution Coefficient in the Two-Phase System. Distribution coefficient for FFA in the two-phase system was calculated from measurements of the initial myristic acid concentration in the aqueous phase prior to addition of si-oil and the myristic acid concentration in the equilibrated aqueous phase using Eq. 4, derived as follows:

FFAs partition between the two phases (aqueous and si-oil) as described by the dimensionless parameter distribution coefficient (D), defined as the ratio of the concentration of FFA in each phase:

$$D = \frac{[FFA]_{oil}}{[FFA]_{aq}} \quad (1)$$

Since the FFA is initially dissolved into the aqueous phase, followed by gravimetric addition of si-oil and equilibration of the two-phase system, the total mass of FFA in the system is conserved as follows:

$$V_{aq} * [FFA]_{initial} = m_{oil} / \rho_{oil} * [FFA]_{oil} + V_{aq} * [FFA]_{aq} \quad (2)$$

Rearranging the mass balance, the concentration of FFA in the oil phase after equilibration can be expressed as:

$$[FFA]_{oil} = \frac{V_{aq}}{m_{oil} / \rho_{oil}} \left([FFA]_{initial} - [FFA]_{aq} \right) \quad (3)$$

Combining Eqs. 1 and 3, the distribution coefficient can be expressed as a combination of known and measurable terms:

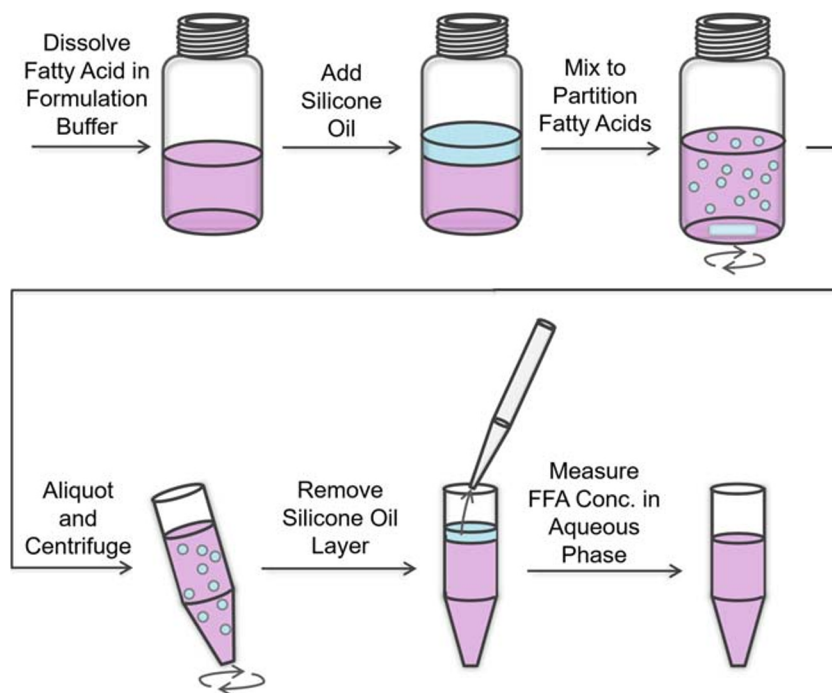
$$D = \frac{V_{aq}}{m_{oil} / \rho_{oil}} \frac{\left([FFA]_{initial} - [FFA]_{aq} \right)}{[FFA]_{aq}} \quad (4)$$

Equation 4 was used directly to measure the distribution coefficient of myristic acid under various experimental conditions. The volume of the aqueous phase and the mass of the added oil phase were fixed. The density of the si-oil used was specified as 0.96 g/mL by the vendor of the material (19). The initial concentration of myristic acid was measured in the aqueous phase prior to addition of si-oil and the final concentration of myristic acid in the aqueous phase was measured post-extraction of the si-oil. Distribution coefficient of myristic acid was measured at a range of aqueous conditions. Finally, a semi-empirical model was developed from the experimental data to predict distribution coefficient at a range of relevant formulation conditions.

Part II: Verification of the Distribution Coefficient Model

Comparison of PS20 Degradation and Free Fatty Acid Particle Formation in Vial and Syringe Configurations. To support practical implications suggested by the FFA distribution coefficient model, semi-representative experiments were performed, using methods adapted from Doshi, *et al.* (20). The time of onset of FFA particle formation upon the degradation of PS20 was compared between siliconized syringes and non-coated glass vials as illustrated in Fig. 2. PS20 was hydrolytically degraded in FB-A. Controlled degradation was performed using the enzymes PCL and CALB. Enzyme working solutions were

Fig. 1 Schematic of methods used to partition fatty acid in a two phase system containing an aqueous phase and a si-oil phase. After overnight partitioning, mixtures were aliquoted into glass centrifuge-safe tubes and centrifuged at 13,200 g to separate the two phases. The si-oil layer was carefully removed from the top of centrifuge tubes using a glass Pasteur pipette.



prepared by dissolving the PCL and/or CALB in FB-A, prior to addition of PS20. PS20 stock solution was prepared at 10% *w/v* in water and spiked into the enzyme working solution to the target initial PS20 concentration.

For each experimental condition, the degrading PS20 solution was distributed into non-coated glass vials and silicone-oil coated syringes immediately after initiation of degradation. After fill, syringes were stoppered using a stopper press. To

ensure maximum contact of si-oil with solution, the stoppers were lowered to within 1 mm of the liquid level and PFSs were stored in the inverted position with the stopper at the bottom. Glass vials were stored upright to avoid contact between the aqueous fill and the stopper. Filled vessels were incubated at 5°C. Concentration of intact PS20 and counts of sub-visible particles $\geq 2 \mu\text{m}$ were monitored over time and compared between vials and PFSs (Fig. 2). It is difficult to visually discern

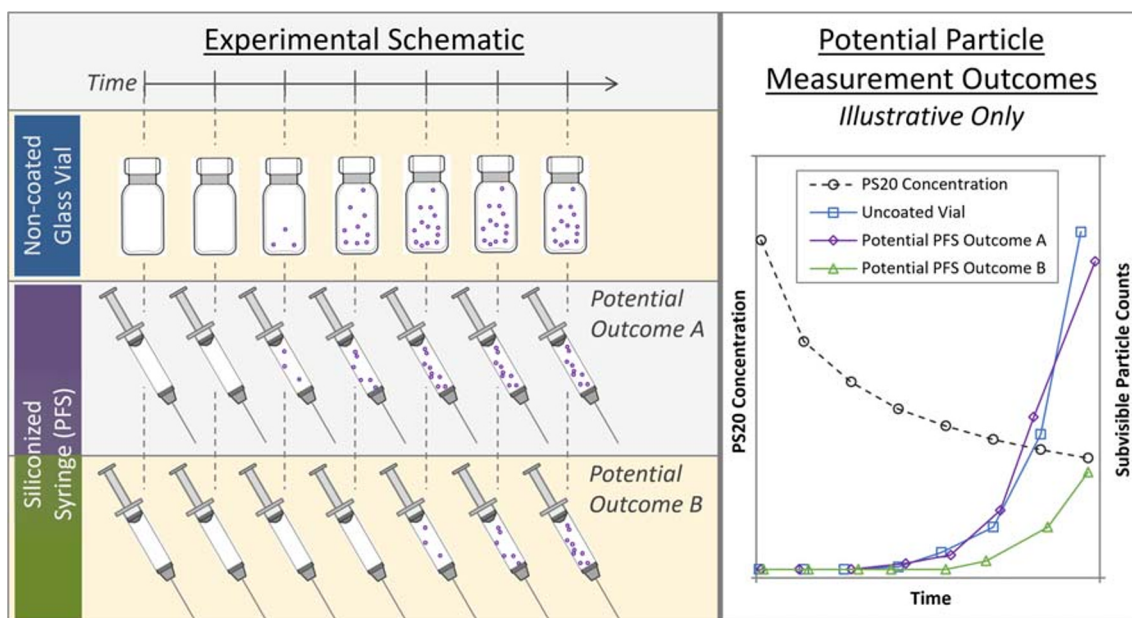


Fig. 2 Schematic of the methods used to compare the time to onset of sub-visible particles between siliconized syringes and non-coated glass vials and the potential outcome of the results. This figure is illustrative only and does not represent actual collected data. Mock data in the particle count plot is displayed with jitter along the time axis to enable easier visualization of the potential outcomes,

particles in the small volume containers studied herein; hence, visual inspection was not performed on the small volume test containers. Instead, for each test condition, a 10 mL aliquot of the degrading mixture was set aside in a large glass scintillation vial and stored at 5°C for visual inspection.

Assays

Free Fatty Acid Quantitation for the Determination of the Distribution Coefficient

FFA concentration measurements were performed using reverse-phase ultra-high performance liquid chromatography (RP-UHPLC) as previously described by Tomlinson *et al.* (9). Chromatography was performed on a Waters Acquity H-Class UHPLC equipped with a Waters Acuity photodiode array (PDA) detector (Milford, MA). FFAs were first derivatized and subsequently separated using a C18 reverse phase column (Acquity BEH300, 1.7 μm , 2.1 \times 150 mm) obtained from Waters (Milford, MA).

Polysorbate 20 Quantitation

PS20 levels were measured by mixed-mode high performance liquid chromatography (MM-HPLC) equipped with evaporative light scattering detection (ELSD), using methods described by Hewitt *et al.* (21). Chromatography was performed on an Agilent 1200 HPLC system equipped with an Agilent 380 ELSD (Palo Alto, CA). PS20 was separated using a mixed-mode cartridge column (OasisMax, 20 \times 2.1 mm, 30 μm) obtained from Waters (Medford, CA). The column was equipped with a Supelco UltraShield pre-column filter, obtained from Sigma Aldrich (St. Louis, MO), to prevent particles from reaching the column.

Polysorbate 20 Component Profile

The distribution of ester species in PS20 was monitored during hydrolytic degradation using reverse-phase high performance liquid chromatography (RP-HPLC) as previously described by Hewitt *et al.* and McShan *et al.* (22,23). Chromatography was performed on an Agilent 1260 HPLC system equipped with an Agilent 1260 ELSD (Palo Alto, CA). PS20 component peaks were separated using a C8 reverse phase column (Zorbax SB, 50 \times 4.6 mm, 5 μm) obtained from Agilent (Palo Alto, CA). With this method, molecule-A co-elutes with PS20 component peaks, interfering with the assay result if it is not removed from solution prior to testing. Therefore, to measure the component profile of PS20 during degradation in solutions containing molecule-A, the protein was first extracted from solution by methanol-induced precipitation. At the desired degradation time point, the degrading solution was treated with sodium succinate and methanol,

then allowed to precipitate for 30 min at -20°C . Precipitate was removed via centrifugation. The remaining supernatant was transferred to a borosilicate glass tube and dried using a Centrivap Centrifugal Vacuum Concentrator equipped with a Centrivap Cold Trap, obtained from LabConco (Kansas City, MO). The dried samples were reconstituted with purified water, then tested using the RP-HPLC assay described.

Measurement of Sub-Visible Free Fatty Acid Particles

Sub-visible particles were counted by flow microscopy. Measurements were performed using a FlowCam Nano system equipped with a 10X objective, 80 \times 570 μm flow cell, and 1 mL syringe pump, obtained from Fluid Imaging Technologies, Inc. (Scarborough, ME). For each measurement, 250 μL of sample was pumped through the flow cell at 250 $\mu\text{L}/\text{min}$ for a total collection time of 60 s. Captured images were classified by particle type (FFA, si-oil, proteinaceous, air bubble, or miscellaneous) based on size and morphology, using previous work by Siska *et al.* and Werk *et al.* (24,25) as guides for particle classification. Examples of classified particle images from the experiments discussed herein are displayed in Fig. 3. All images not classified as FFA particles were excluded from analysis. As si-oil is known to desorb from coated PFS surfaces and form particle-like droplets, baseline differences in total sub-visible particles between PFSs and vials were removed by excluding si-oil droplets from analysis. The si-oil baseline remained relatively flat and low (data not shown) across the experimental time frame and did not show a clear correlation with fatty acid particle counts.

RESULTS AND DISCUSSION

Part I: Free Fatty Acid Distribution Coefficient Model

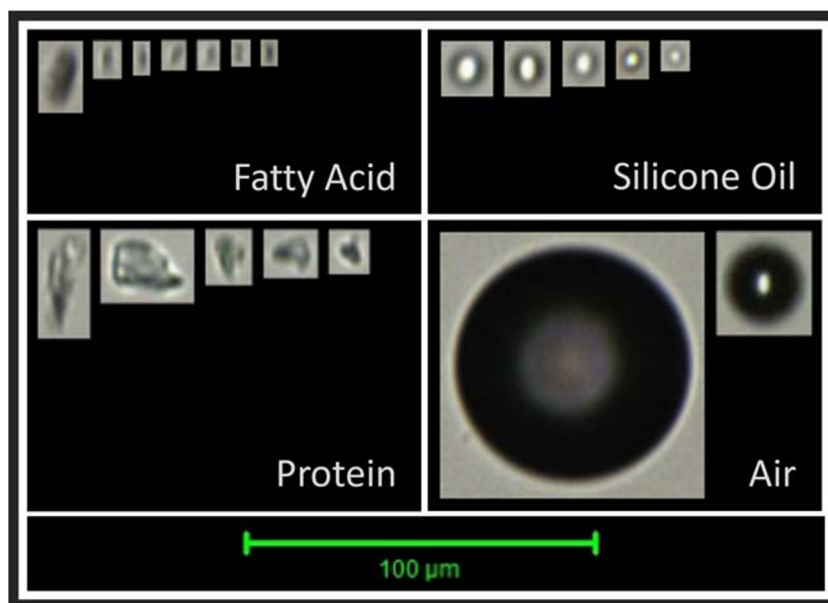
Developing the Distribution Coefficient Model

As previously hypothesized, si-oil can act as a sink for FFAs in DP solutions pre-filled into coated syringes. The efficiency of FFA sequestration from aqueous solution is defined by the partitioning of the FFAs from solution into the si-oil phase. If partitioning does occur, the magnitude of the partitioning effect determines the extent to which si-oil coatings can prevent or delay FFA particle formation for susceptible DPs.

A simple mathematical model for the distribution coefficient was derived to predict partitioning behavior of FFAs in the two-phase system. The simplified model system is visually represented in Fig. 4, showing all possible distribution behavior potentially occurring in the system.

The distribution coefficient (D), defined as the ratio of the sum of the concentration of all forms of the FFA (ionized and

Fig. 3 Flow microscopy images of various particles, qualitatively sorted by type based on particle morphology.



un-ionized) between the two phases, describes the FFA partitioning behavior:

$$D = \frac{[FFA]_{oil}}{[FFA]_{aq}} = \frac{[HA]_{oil} + [A^-]_{oil}}{[HA]_{aq} + [A^-]_{aq}} \quad (5)$$

As a highly non-polar organic polymer, si-oil is unlikely to solubilize the ionized form of FFA. Applying this assumption, the distribution coefficient is simplified:

$$D = \frac{[HA]_{oil}}{[HA]_{aq} + [A^-]_{aq}} \quad (6)$$

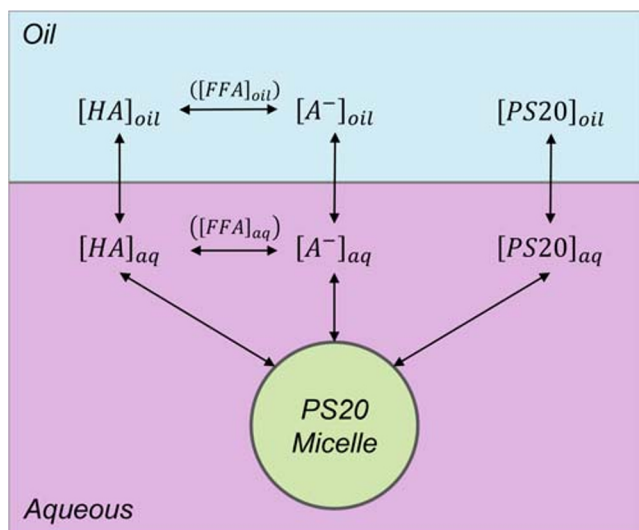


Fig. 4 Schematic of the possible distribution behavior of free fatty acid in a two phase system with an aqueous phase containing PS20 and a si-oil phase.

The behavior of only the un-ionized form of the FFA in the two phase system can be described by the partition coefficient, defined as the ratio of the concentration of the un-ionized form between the two phases:

$$P_{oil/aq}^{HA} = \frac{[HA]_{oil}}{[HA]_{aq}} \quad (7)$$

Combining Eqs. 6 and 7, the distribution coefficient can be expressed in terms of the aqueous mole fraction of the un-ionized form of the FFA and the partition coefficient of the un-ionized FFA:

$$D = \frac{[HA]_{oil}}{[HA]_{aq} + [A^-]_{aq}} * \frac{[HA]_{aq}}{[HA]_{aq}} = \frac{[HA]_{aq}}{[HA]_{aq} + [A^-]_{aq}} * \frac{[HA]_{oil}}{[HA]_{aq}} \\ = x_{HA,aq} * P_{oil/aq}^{HA} \quad (8)$$

The mole fraction of un-ionized FFA in the aqueous phase can be described by the Hendersen-Hasselbalch equation:

$$x_{HA,aq} = \frac{1}{1 + 10^{pH - pK_a}} \quad (9)$$

Combining Eqs. 8 and 9, the distribution coefficient for FFA in the two phase system can be described as:

$$D = \frac{P_{oil/aq}^{HA}}{1 + 10^{pH - pK_a}} \quad (10)$$

In eq. 10, the primary variable affecting distribution coefficient is the pH of the formulation. The exchange between ionized and un-ionized FFA species in the aqueous phase is driven by the pH of the solution. The aforementioned assumption that the ionized form of FFA does not appreciably

partition into the si-oil phase would suggest that the ratio of the two species in the aqueous phase would likely have an impact on the overall ability for the si-oil to act as a sink for FFA species as a whole.

In addition to pH, another formulation-relevant parameter expected to impact FFA distribution coefficient is the PS20 concentration of the aqueous solution. Previous work by Doshi *et al.* suggests that micelles formed by PS20 in aqueous solution at concentrations above its CMC can uptake FFAs (13). In the described two-phase system, PS20 micelles within the aqueous phase may act as an additional sink for FFA species (Fig. 4). With increasing PS20 concentration, the increased presence of PS20 micelles may drive the partitioning of un-ionized FFAs away from the si-oil phase and towards the aqueous phase.

Together, it is therefore expected that the distribution coefficient should be a function of aqueous pH and PS20 concentration. Unlike pH, the relationship between FFA distribution coefficient and PS20 concentration is difficult to model. Instead, this relationship was determined empirically, as explained later in this work.

Semi-Empirical Modeling of the Distribution Coefficient for Myristic Acid

Myristic acid was selected as a model FFA for distribution coefficient measurements. In biopharmaceutical formulations containing PS20, myristic acid released upon hydrolytic degradation of the surfactant poses a higher risk of particle formation relative to most other FFA degradation byproducts. Previous work by Saggu *et al.* identified myristic acid and palmitic acid as the primary constituents of particles present in two different aged antibody formulations containing PS20 (14). Of the two, distribution of only myristic acid was measured herein because the RP-UHPLC method used to quantify FFAs is not sensitive enough to reliably measure distribution of the relatively less soluble palmitic acid.

The distribution coefficient for myristic acid was measured in solutions at a range of pH values and PS20 concentrations that span typical biopharmaceutical formulation conditions. First, to understand the univariate impact of aqueous pH on the distribution coefficient, measurements were taken in formulation buffer-A (FB-A) at pH values ranging from approximately 5.2 to 7.5, while maintaining all other parameters as constant. These samples used a constant PS20 concentration of 0.04% (*w/v*), which is representative of levels in biopharmaceutical formulations. The ratio of si-oil to aqueous phase was maintained at 50 mg/mL, far in excess of si-oil to aqueous fill ratios typical of PFSs, selected to enable measurement of partition coefficient despite assay limitations rather than to be representative. The phase ratio does not impact distribution coefficient, as will be discussed later.

As hypothesized, the distribution coefficient correlates with pH (Fig. 5a). Using non-linear regression, the experimental data were fit to Eq. 10. At the specified PS20 concentration, the partition coefficient of the un-ionized myristic acid species ($P_{oil/aq}^{HA} |_{0.04\%PS20}$) is assumed constant and independent of pH. Further, the pKa of myristic acid is assumed constant and independent of both pH and PS20 concentration, as it has been previously reported that pKa of small molecules is independent of micellar concentration of non-ionic surfactants (26,27). Finally, all experimental runs are considered to be independent. The best fit estimates of the parameters $P_{oil/aq}^{HA}$ and pKa are summarized in Table I. The best fit curve and the 95% confidence interval curve is graphically represented in Fig. 5a. The best fit of the experimental data to the mathematical model produces the relationship:

$$D |_{0.04\%PS20} = \frac{P_{oil/aq}^{HA} |_{0.04\%PS20}}{1 + 10^{pH-pKa}} = \frac{45.90}{1 + 10^{pH-6.88}} \quad (11)$$

Distribution coefficient as a function of pH closely fits the relationship expressed by Eq. 11. All data points fall within the 95% confidence interval curves of the fit and the standard errors of both fit parameters are well below 10% of the best fit estimated values. The myristic acid pKa of 6.9 as determined by the fit of the distribution data closely matches the value 6.7 previously reported by Doshi *et al.*, providing further confidence in the fit (13).

The distribution coefficient of myristic acid decreases with increasing pH as expected, suggesting that the ability for si-oil to aid in the mitigation of FFA particle formation is greatest for DPs formulated at low pH. The ratio of un-ionized to ionized FFA decreases with increasing pH, thus driving FFA species away from the si-oil phase over to the aqueous phase. The impact of the ionization behavior is particularly pronounced at pH near the pKa, a property that is reflected by the observed inflection point of the s-shaped best fit model. The distribution coefficient of myristic acid plateaus below approximately pH 6, suggesting there is minimal increase to the distribution coefficient at pH conditions below the lower end of the tested range.

Equation 11 can predict myristic acid distribution at any pH in formulations containing 0.04% (*w/v*) PS20. To account for the impact of aqueous PS20 concentration, the distribution coefficient was measured for myristic acid in FB-A at different PS20 concentrations, ranging from 0.01% to 0.06% (*w/v*). All other parameters including pH were kept constant. In the absence of a mechanistically derived relationship between distribution coefficient and PS20 concentration, an empirical relationship was determined using a pH at which both FFA species were present in solution. Measurements were performed using samples at a pH of 6.6, which is close to the pKa value of myristic acid, as reported in literature and

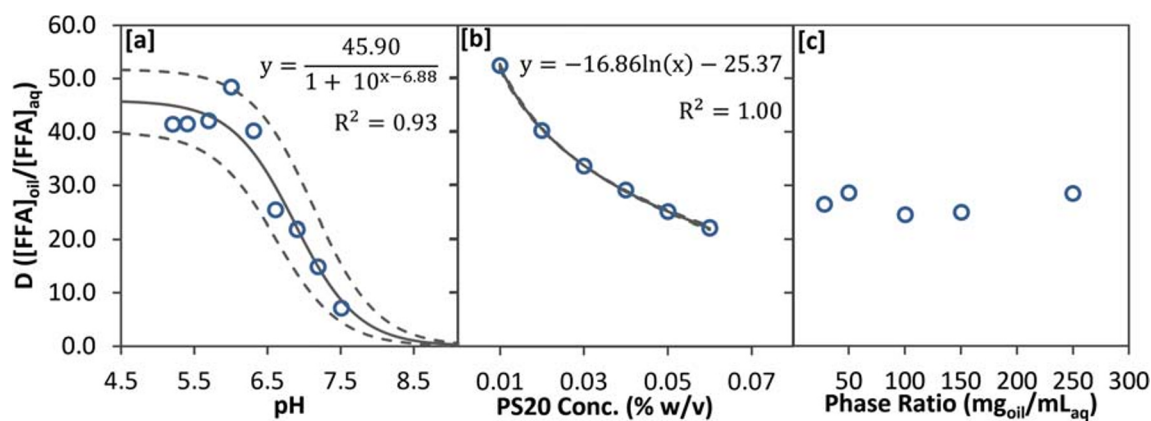


Fig. 5 Distribution coefficient for myristic acid as a function of (a) pH (at 50 mg_{oil}/mL_{aq}, 0.04% PS20), of (b) PS20 concentration (at 50 mg_{oil}/mL_{aq}, pH 6.6), and of (c) ratio of si-oil phase to aqueous phase (at pH 6.6, 0.04% PS20). Measured data points are shown by the open circles. Solid lines show the best fit line, described by the equation and R² value captured within the corresponding panel of the plot. Dotted lines show 95% confidence interval about the best fit line.

as predicted by the best fit model expressed by Eq. 11. At this pH, both the ionized and the un-ionized species of myristic acid are present in the aqueous solution at near equal levels. As in the previous pH experiment, the ratio of si-oil mass to aqueous volume was maintained at 50 mg/mL, far in excess of si-oil to aqueous fill ratios typical of PFSs.

As expected, the distribution coefficient of FFA into si-oil decreases with increasing PS20 concentration (Fig. 5b). The relationship between PS20 concentration and distribution coefficient is non-linear in the range of 0.01% - 0.06% w/v PS20. In the absence of a mechanistically derived mathematical relationship, the data were empirically fit to the following equation:

$$D|_{pH\ 6.6} = -16.86 * \ln([PS20]) - 25.37 \quad (12)$$

where:
[PS20] is in units %w/v

The relationship should be verified if applied to PS20 concentrations beyond the tested range. Of particular note, the low end of the tested range of PS20 concentration is close to the critical micelle concentration (CMC) of approximately 0.002% w/v (5,28). As the concentration of PS20 approaches its CMC, the relative amount of PS20 molecules found in micellar structures compared to the amount present at interfacial surfaces decreases. Therefore, particular care must be exercised when considering application of the empirically

derived relationship to formulations near or below the CMC of PS20.

Combining Eqs. 11 and 12 allows the estimation of the distribution coefficient at any combination of pH and PS20 concentration. To develop this combined expression, Eq. 11 was first used to obtain the distribution coefficient at the desired pH at a reference point of 0.04% PS20. To translate this distribution coefficient to any desired PS20 (w/v) concentration, a ratio R was calculated from Eq. 12. R is defined as the ratio of the distribution coefficient at the desired PS20 concentration to the distribution coefficient at the reference PS20 concentration (0.04% w/v).

$$R = \frac{-16.86 * \ln([PS20]) - 25.37}{-16.86 * \ln(0.04) - 25.37} \quad (13)$$

R is expected to be independent of pH. PS20 is a nonionic surfactant, so the ability for PS20 to solubilize FFAs is not expected to be pH dependent. R is subsequently multiplied by Eq. 11 to yield the distribution coefficient at the desired aqueous conditions:

$$D = \frac{P_{oil/aq}^{HA} \Big|_{0.04\% PS20} * \frac{-16.19 * \ln([PS20]) - 24.35}{-16.19 * \ln(0.04) - 24.35}}{1 + 10^{pH - pKa}} \quad (14)$$

or, simplified:

$$D = \frac{-26.77 * \ln([PS20]) - 40.26}{1 + 10^{pH - 6.88}}$$

Table 1 Parameter Estimates for the Best-Fit Regression of Distribution Coefficient as a Function of pH at a Constant PS20 Concentration of 0.04% w/v

Parameter	Estimate	Std. Error	Lower Limit	Upper Limit
$P_{oil/aq}^{HA} \Big _{0.04\% PS20}$	45.90	2.48	40.03	51.78
pKa	6.88	0.11	6.62	7.14

This semi-empirical relationship described by Eq. 14 is graphically represented in Fig. 6a and can be used to predict the equilibrium distribution coefficient of myristic acid in the two-phase system containing si-oil and FB-A at a range of pH and PS20 concentrations. Distribution coefficient is highest at low pH and low PS20 concentration, suggesting that any benefit that si-oil has towards the mitigation of PS20-related FFA particle formation is greatest for such formulations.

The partition coefficient determined here for myristic acid in the described si-oil/aqueous/PS20 system (45.9 or $10^{1.7}$, Table I) is on the order of the partition coefficient previously reported for myristic acid in a similar oil/water system. Bravo *et al.* reported a partition coefficient of $10^{2.3}$ for myristic acid in a heptane/water system, notably measured without surfactant in the aqueous phase (29). $P_{\text{octanol/water}}$ for heptane and for hexyldimethylsiloxane (a subspecies of si-oil) have both been reported on the order of 10^4 , suggesting similar hydrophobicity for the two oils (30,31). As these two oil phases are comparable in hydrophobicity, it is expected that myristic acid will partition to a similar extent in each of the aforementioned systems.

To better compare the value reported by Bravo *et al.* to the results obtained herein, it is useful to approximate the partition coefficient of myristic acid in the si-oil/aqueous system in the absence of PS20, as surfactant concentration was shown to impact partitioning behavior (Fig. 5b). As previously discussed, the observed relationship between PS20 concentration and distribution behavior is likely driven by the uptake of non-ionized FFA species into PS20 micelles in the aqueous phase. It follows that the partition coefficient of myristic acid in the absence of PS20 is likely to be closely approximated by its value at the CMC of PS20. To approximate this value, the ratio R (Eq. 13) was evaluated at the CMC of PS20 (0.002% *w/v*) and multiplied by the partition coefficient value reported in Table I. This results in an approximated partition

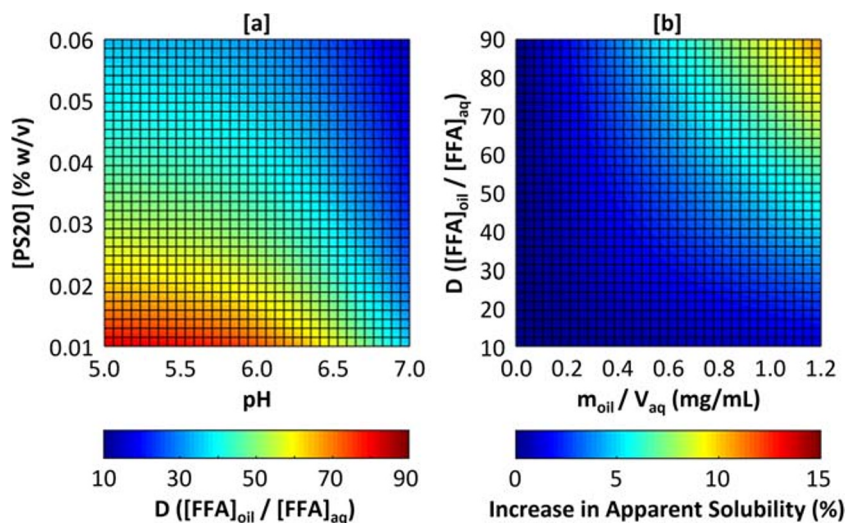
coefficient of $10^{2.1}$ for myristic acid in a si-oil/water system with no PS20, comparable to the $10^{2.3}$ value reported by Bravo *et al.* in the heptane/water system.

Underlying Assumptions to the Distribution Coefficient Model

An underlying assumption in the experimental determination of the myristic acid distribution coefficient is the independence of the distribution coefficient from the relative amounts of the two phases present. The experiments conducted to develop the semi-empirical model were performed at a si-oil-to-aqueous-phase ratio of 50 mg/mL which is in excess to ratios typical of PFSs. Bake-on siliconization processes for PFSs result in si-oil levels of <0.1 mg/barrel, while the spray-on siliconization process result in levels 0.2–1.0 mg/barrel for a standard 1 mL long syringe (32). This translates to a maximum si-oil to aqueous-volume ratio of 1 mg/ml, which is far exceeded by the 50 mg/mL phase ratio used in the distribution coefficient experiments. The use of a ratio in excess of the typical PFS ratio was necessary to produce a measurable change in the FFA concentration pre- and post- partitioning, due to limitations in the sensitivity of the FFA quantification assay. The assumption of independence between distribution coefficient and phase ratio is, thus, paramount in applying the empirical model to the PFS use case.

To verify this assumption, the distribution coefficient for myristic acid was measured at various ratios of si-oil mass to aqueous phase volume, while keeping all other conditions constant. PS20 concentration was maintained at 0.04% *w/v* and pH at 6.6. The volume of aqueous phase was held constant at 2 mL, while the mass of si-oil was varied from 60 mg to 500 mg (30 mg/mL to 250 mg/mL phase ratio). The distribution coefficient of myristic acid remains constant with the change in phase ratio (Fig. 5c). This result suggests that distribution coefficient is independent of the phase

Fig. 6 Distribution coefficient of (a) myristic acid as a function of pH and PS20 concentration and (b) increase in apparent solubility as a function of phase ratio and distribution coefficient. Distribution coefficient was predicted using the semi-empirical model expressed by Eq. 14. Increase in apparent solubility was predicted using the model expressed by Eq. 20.



ratio and can be generalized across any ratio of the phases.

Another assumption of the distribution coefficient model is that PS20 concentration and pH are the only two factors affecting the distribution coefficient of myristic acid in the aforementioned two phase system. The model does not account for potential impacts of the concentration or identity of other aqueous solution components (i.e. buffers, salts, or sugars). Further, the model was constructed using data generated in the absence of a protein therapeutic. Distribution behavior is largely driven by differences in FFA solubility in each of the phases. It has previously been demonstrated that aqueous FFA solubility is not affected by the presence of a monoclonal antibody (mAb) in a range of 10–90 mg/mL (13). This suggests that the presence (and concentration) of mAb or other mAb-like proteins is not expected to have a major impact on the distribution model. However, depending on the hydrophobicity of the formulated protein, it may be possible for FFA-protein interactions to occur such that the solubility of FFA in aqueous solution is impacted and, as a result, the distribution behavior of FFA is impacted. As FFA-protein interactions would improve FFA solubility in the aqueous phase, such impact would be expected to decrease to the distribution coefficient further reducing the benefit of si-oil to FFA particle formation.

Another important assumption is that the mathematical model described by Fig. 6 and Eq. 14 does not explicitly consider interfacial interactions that may be occurring to sequester FFA away from the bulk aqueous phase. As FFAs are amphipathic molecules, it is possible that FFAs are sequestered from the bulk phases in an oil/aqueous system via surface adsorption, due to interfacial phenomena at the phase boundary. The methods used to experimentally measure distribution coefficient (Fig. 1) rely only on measurement of FFA in the aqueous phase, capturing the sum total of removal of FFA from the aqueous phase (whether by partitioning behavior or by interfacial interaction). It is possible, therefore, that distribution coefficient values calculated using Eq. 4 are overestimates of the true values.

Practical Implications of the Free Fatty Acid Distribution Coefficient Model

The semi-empirical distribution coefficient model demonstrates that si-oil does have some capacity to act as a sink for FFAs. However, the extent of this partitioning effect is key to understanding implications to the risk of PS20-related FFA particle formation for DPs filled in si-oil coated vessels. To understand such implications of the model, an equation was developed to determine the total capacity of a given system for solubilizing FFA. The ‘apparent FFA concentration’ in the aforementioned two phase system is defined as the total mass

of FFA in all phases divided by the volume of the aqueous phase alone, as expressed by the following equation:

$$[FFA]_{app} = \frac{m_{FFA,aq} + m_{FFA,oil}}{V_{aq}} \quad (15)$$

or

$$[FFA]_{app} = [FFA]_{aq} \left(1 + \frac{m_{FFA,oil}}{m_{FFA,aq}} \right)$$

Rearranging the definition for the distribution coefficient (Eq. 1):

$$D = \frac{[FFA]_{oil}}{[FFA]_{aq}} = \frac{m_{FFA,oil}/V_{oil}}{m_{FFA,aq}/V_{aq}} = \frac{m_{FFA,oil}}{m_{FFA,aq}} * \frac{V_{aq}}{V_{oil}} \quad (16)$$

Combining Eqs. 15 and 16:

$$[FFA]_{app} = [FFA]_{aq} \left(1 + D * \frac{V_{oil}}{V_{aq}} \right) \quad (17)$$

At the solubility limit of myristic acid in the aqueous phase, the apparent system solubility of myristic acid can thus be expressed as:

$$S_{FAA,app,aq} = S_{FAA,aq} \left(1 + D * \frac{V_{oil}}{V_{aq}} \right) \quad (18)$$

By the above equation, the apparent FFA solubility in a system containing si-oil is dependent only on the distribution coefficient and on the phase ratio. Applying this relationship to a practically relevant parameter, the percent increase in the apparent solubility of FFA due to the presence of si-oil can be defined as:

$$\% \text{Increase in Apparent Solubility} = \frac{S_{App,FFA,aq} - S_{FFA,aq}}{S_{FFA,aq}} * 100 \quad (19)$$

Combining with Eq. 18:

$$\% \text{Increase in Apparent Solubility} = \frac{\left(S_{FFA,aq} + D * S_{FFA,aq} * \frac{V_{oil}}{V_{aq}} \right) - S_{FFA,aq}}{S_{FFA,aq}} * 100$$

Simplifying and considering oil on a mass basis, as is typical with PFS specifications:

$$\% \text{Increase in Apparent Solubility} = D * \left(\frac{m_{oil}}{V_{aq}} \right) * \rho_{oil}^{-1} * 100 \quad (20)$$

The increase in apparent solubility of myristic acid as a function of distribution coefficient and phase ratio is graphically represented in Fig. 6b. As expected, the increase in apparent solubility is maximized at a high ratio of si-oil to aqueous phase and at aqueous conditions that result in high distribution coefficient (low pH and low PS20 levels). Within the

model design space (0.01–0.10% *w/v* PS20, pH 5.0–7.5) and at the highest ratio of si-oil to aqueous phase typical of PFSs (1 mg/mL, as previously mentioned), the maximum percent increase in apparent myristic acid solubility predicted by the model is 8.5%. This prediction may be an over-estimation of the benefit of si-oil in typical PFSs, considering the strong driver to minimize si-oil levels in PFSs to protect proteins against si-oil induced aggregation (33).

Part II: Verification of the Distribution Coefficient Model

Hydrolytic Degradation of PS20 Using Model Lipases

To corroborate the apparent solubility predictions derived from the distribution coefficient model, the time of onset of sub-visible particle formation upon hydrolytic degradation of PS20 was compared between PFSs and vials (Fig. 2). To perform this comparison, a consistent and relatively quick method to hydrolytically degrade PS20 was needed. Previous work by McShan, *et al.* demonstrated that the lipases CALB and PCL degrade PS20, while displaying differing selectivity towards the various ester species that comprise PS20 (23). A number of combinations of these two lipases were screened to identify a ratio at which PS20 is degraded with no particular selectivity towards any of its comprising esters. Combinations were initially screened in FB-A at a relatively high initial concentration of 0.1% *w/v* PS20. Qualitatively, degradation of all PS20 component ester species were observed at a PCL: CALB ratio of 6000:1 U:U (Fig. 7).

Additional tests were performed to verify whether the observed PS20 degradation profile remains fairly consistent with scaling of the initial PS20 concentration. The degradation profile remains consistent in the range of 0.02–0.10% *w/v* initial PS20 (Fig. 8a, c, and d). Testing was not performed below an initial PS20 concentration of 0.02% *w/v*, due to limitations in the sensitivity of the assay, but the profile is expected to remain consistent at lower initial PS20 concentrations. The degradation profile was further assessed in the presence of 100 mg/mL molecule-A, to verify that no interactions occur between enzyme and molecule-A such that the activity of the enzymes is impacted. The degradation profile is maintained in the presence of 100 mg/mL molecule-A (Fig. 8b). Any trace enzymes that may be present in the molecule-A drug substance are insignificant in concentration relative to the large amounts of CALB and PCL used and, therefore, do not affect this assessment.

Comparison of Degradation Rate and Onset of Particle Formation in PFS and Vial Configurations

Based on the screening results, the 6000:1 U:U ratio of PCL to CALB was selected and used for the vial *vs.* PFS experiments.

Difference in onset of particle formation time was assessed between degrading solutions in PFSs and glass vials using this lipase cocktail. PFSs were filled to low volume to maximize the ratio of si-oil to aqueous phase and aqueous conditions of low pH and PS20 concentration (pH 5.0, 0.01% *w/v* PS20) were selected to maximize FFA distribution coefficient. Both measures were intended to maximize the potential to produce a discernable difference in particle onset time.

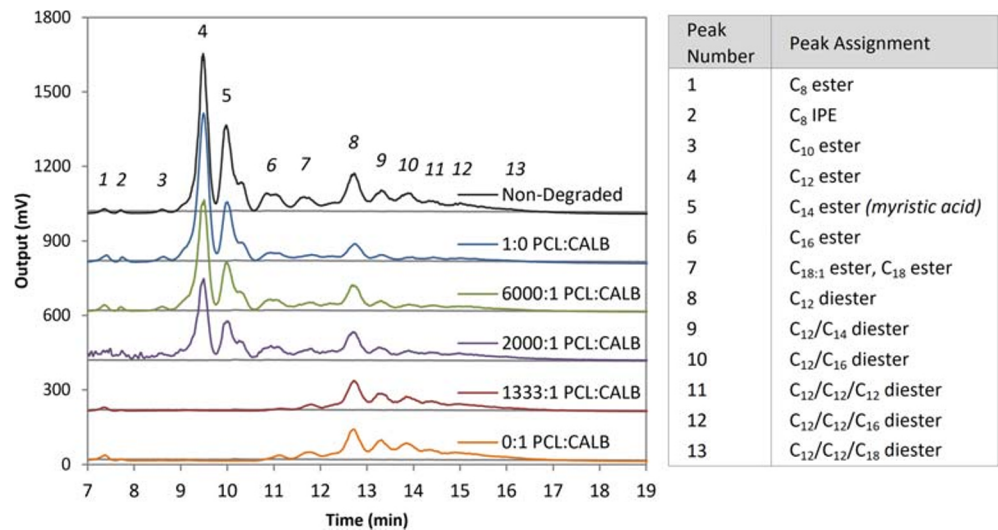
PFS-A was used as a representative-case PFS in terms of si-oil to fill volume. Considering the nominal si-oil-to-volume ratio for PFS-A (0.026 mg si-oil per mL of aqueous fill), the distribution coefficient model predicts an increase in apparent myristic acid solubility of only 0.2% at the selected aqueous conditions. The absolute fill volume and mass of si-oil coating for PFS-A are confidential, but conclusions can be drawn from the relative amounts of the two phases.

PFS-B (average si-oil coating of 0.7 mg/barrel) was included in the study as a better-case PFS in terms of the ratio of si-oil to fill volume, and was filled to 0.5 mL out of its 2.25 mL nominal volume. Under the extreme best-case assumption that the stoppering process exposes the aqueous fill to the entirety of the si-oil coating for PFS-B (1.4 mg si-oil per mL of aqueous fill), the model predicts 11.9% increase in apparent myristic acid solubility for the better-case syringe. However, it is unlikely that the fill is exposed to levels of si-oil at this extreme best-case. Rather, the true ratio of si-oil to aqueous volume is expected to be nearer to the nominal si-oil to volume ratio (0.3 mg si-oil per mL of aqueous fill), at which the model predicts a 2.7% increase for PFS-B. We expect the results presented below should be repeatable for any PFS system in which the si-oil levels are at or below those specified for best-case PFS-B.

Using the lipase cocktail, no difference is observed in overall rate of PS20 degradation between the non-coated glass vial and the PFS configuration for either PFS-A or PFS-B in the absence of molecule-A (Fig. 9a and b). Further, no difference is observed between vial and PFS-A at several additionally tested protein concentration levels, to a maximum of 100 mg/mL molecule-A (Fig. 9c and d). This demonstrates that differences in the physical properties of the vessels do not affect the kinetics of the enzyme mixture used. The results also demonstrate an independence from protein concentration, providing evidence that molecule-A does not influence the interaction between PS20 and the model lipases, up to the tested concentration of 100 mg/mL molecule-A. This provides confidence that the results of the particle formation experiments are not confounded by unintended differences in enzymatic activity between the test cases.

No difference is observed in the onset of ≥ 2 μm FFA sub-visible particle formation between the PFS and non-coated glass vial in the absence of molecule-A for both PFS-A and PFS-B (Fig. 9a and b). Further, no difference is observed in the onset of FFA particle formation between PFS-A and the glass

Fig. 7 PS20 component profiles upon degradation of 0.1% PS20 with various ratios of the lipases PCL and CALB. Displayed ratios of the enzymes are in U:U. Reactions were performed at 5°C in glass HPLC vials with a fill volume of 1 mL. The chromatograms were captured after approximately 90 min of degradation.



vial at additionally tested protein concentration levels, to a maximum of 100 mg/mL molecule-A (Fig. 9c and d). The time to onset of sub-visible particle formation varies slightly from experiment to experiment, though there is no difference between PFS and vial within any experiment. For all the formulations, a separate study arm in larger glass scintillation vials showed that the onset in sub-visible particle formation preceded visual observation of particles (under black and white background) by approximately 30–40 min. Given the subjective nature of visible particle identification, and the

challenge of visual inspection of small volume containers (such as PFSs), only the more sensitive output of sub-visible particle counts was used to directly compare between vial and PFS.

While the results suggest that si-oil coatings on the interior walls of the two PFSs studied are not likely to provide mitigation against FFA particle formation, it is important to consider the limitations of the work presented. The model lipases used in this study are not endogenous to cell types most commonly used as hosts for biopharmaceutical production and, therefore, may not be truly representative of the trace lipases that

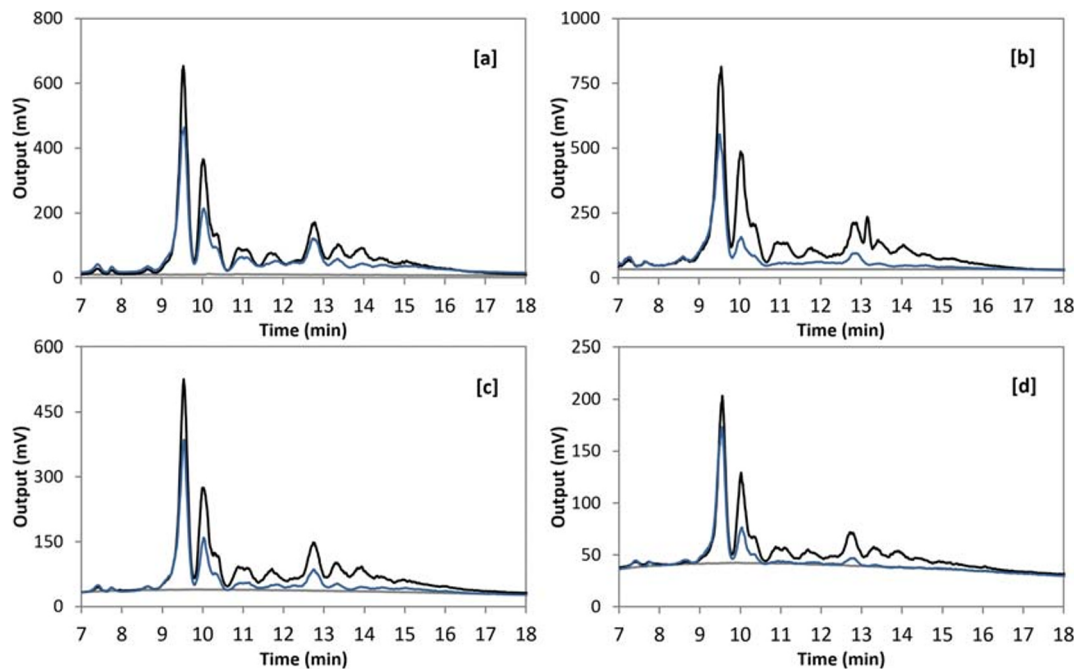


Fig. 8 Degradation using 6000:1 PCL:CALB at various PS20 concentrations, and in the absence and presence of molecule-A. Black traces are the un-degraded control for each condition. Grey traces are blank injections. Test conditions represented in each panel: **(a)** 0.1% PS20 without molecule-A, measured after 84 mins of degradation. **(b)** 0.1% PS20 with 100 mg/mL molecule-A, measured after 75 mins of degradation. **(c)** 0.04% PS20 without molecule-A, measured after 95mins of degradation. **(d)** 0.02% PS20 without molecule-A, measured after 254 mins of degradation.

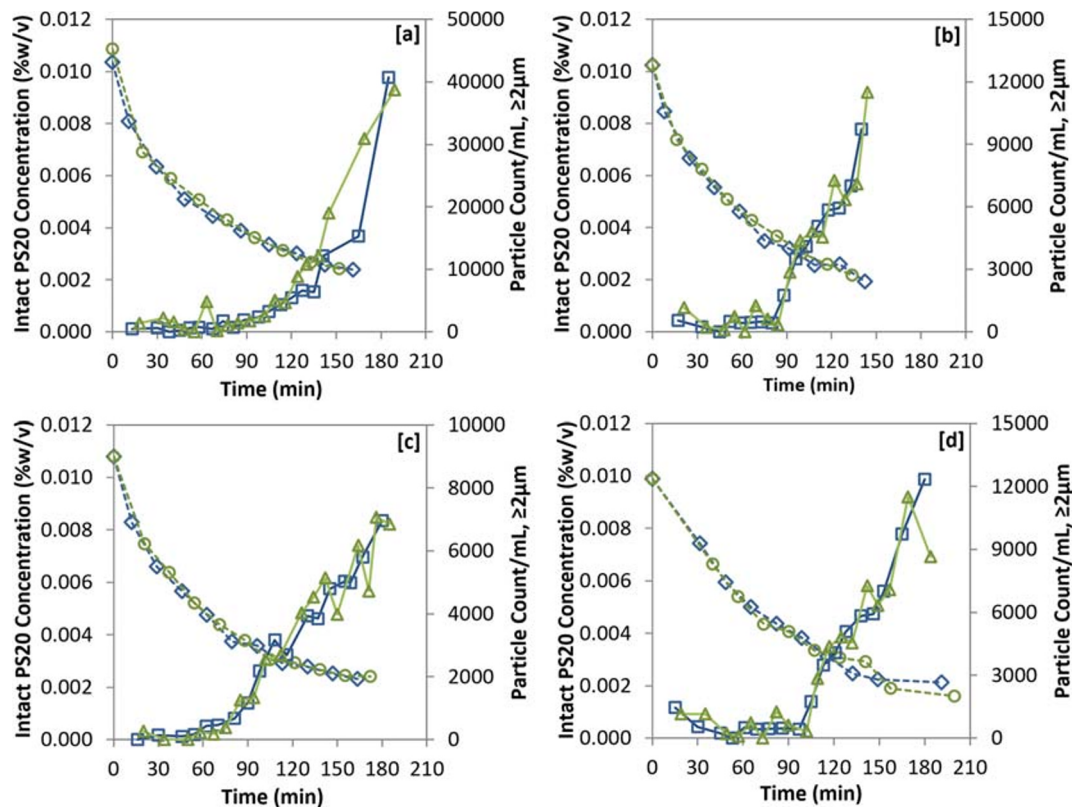


Fig. 9 Comparison of PS20 degradation rate as measured by HPLC-ELSD and time to onset of sub-visible fatty acid particles as measured by flow microscopy for various test conditions. PS20 concentration is depicted by blue diamonds for degradation performed in vials and by green circles for degradation performed in PFSs. Baseline-corrected particle counts are depicted by blue squares for degradation performed in vials and by green triangles for degradation performed in PFSs. Test conditions represented in each panel: (a) = PFS-A, 0 mg/mL molecule-A. (b) = PFS-B 0 mg/mL molecule-A. (c) = PFS-A, 40 mg/mL molecule-A. (d) = PFS-A, 100 mg/mL molecule-A.

may be present in actual DPs. The specificity of the lipase cocktail used for the accelerated degradation experiments likely differs from the specificity of the lipase(s) that may be present in actual DPs. Lipase specificity has a direct impact to the relative abundance of the various PS20 species remaining after a period of degradation (20). Micellar behavior and morphology differ for the various ester species comprising PS20, so it is likely that the distribution of ester species affects the ability for PS20 to increase aqueous FFA solubility (34,35).

It is also important to consider that the conclusions drawn from this work are specific to PS20. The ester distribution and micellar properties of Polysorbate 80 (PS80), another commonly used surfactant in biopharmaceutical formulations, differ from PS20 (5). Though myristic acid was selected as a model FFA for PS20 degradation, it is likely that oleic acid carries more significance for PS80. Oleate esters are the most abundant ester in PS80, but make up only 5.1% of esters in HP grade PS20 (5,20). Oleic acid, unlike myristic acid, is an unsaturated fatty acid with a cis double bond which may impact its partitioning behavior into silicone oil.

Finally, one must consider the time frame over which the particle formation experiments were conducted. Factors involved either in the partitioning of FFAs or in the nucleation

of FFA particles could require the relatively longer timeframes relevant to DP storage and be missed by the accelerated nature of the presented degradation experiments.

CONCLUSION

PS20 is widely used in biopharmaceutical DPs to protect protein against interfacial stresses. Enzymes endogenous to the host cells may co-purify with the target protein and be present at trace levels in DPs. These enzymes can hydrolytically degrade PS20, releasing FFAs as a byproduct of the degradation. For some products, the accumulation of FFAs can result in the formation of particles, affecting long term stability and shelf life. It is hypothesized that the si-oil coated on the interior of PFSs may act as a sink to FFAs generated upon hydrolytic degradation of PS20, providing some risk mitigation against FFA particle formation for DPs particularly susceptible to this risk.

A semi-empirical model was built to predict the distribution coefficient for myristic acid as a function of pH and PS20 concentration in a two phase system containing a si-oil phase and an aqueous phase. The model was used to estimate the

increase in apparent solubility of myristic acid due to the presence of si-oil for PFS systems at formulation relevant aqueous conditions. The results suggest that the si-oil present in PFSs offers modest benefit to apparent myristic acid solubility, maximized in vessels with high levels of si-oil and for formulations at low pH and with a low initial PS20 level. However, the partitioning of FFAs into si-oil is unlikely to result in practically meaningful or measurable difference in FFA particle formation rate at typical biopharmaceutical formulation conditions and at si-oil levels found in typical PFSs.

The results suggested by the model were verified in semi-representative particle formation experiments. Accelerated hydrolytic degradation of PS20 was performed using a combination of commercially available lipases, targeting all ester species of PS20 with no particular selectivity. For various tested conditions, degrading mixture was aliquoted into si-oil coated PFSs and non-coated glass vials, then monitored by flow microscopy for the onset of $\geq 2 \mu\text{m}$ sub-visible particle formation. No measurable difference was observed in the onset of particles between PFS and vial for two models of siliconized syringes and in formulations at 0, 40, and 100 mg/mL of the protein molecule-A. The results of the model and the semi-representative experiments together suggest that FFAs do partition into the si-oil coated on the interior walls of PFSs, but the extent of the partitioning effect does not offer significant mitigation to the risk of FFA particle formation in DPs susceptible to hydrolytic degradation of PS20.

ACKNOWLEDGMENTS AND DISCLOSURES. The authors would like to acknowledge the efforts of Miguel Saggu and Anthony Tomlinson for assistance with sub-visible particle analysis and FFA quantitation. The authors would also like to acknowledge Vikas Sharma and Tom Patapoff for their insights and discussions.

REFERENCES

- Manning MC, Patel K, Borchardt RT. Stability of protein pharmaceuticals. *Pharm Res*. 1989;6(11):903–18.
- Duncan MR, Lee JM, Warchol MP. Influence of surfactants upon protein/peptide adsorption to glass and polypropylene. *Int J Pharm*. 1995;120(2):179–88.
- Wang W. Instability, stabilization, and formulation of liquid protein pharmaceuticals. *Int J Pharm*. 1999;185(2):129–88.
- Jorgensen L, Hostrup S, Moeller EH, Grohganz H. Recent trends in stabilising peptides and proteins in pharmaceutical formulation – considerations in the choice of excipients. *Expert Opin on Drug Delivery*. 2009;6(11):1219–30.
- Kerwin BA. Polysorbates 20 and 80 used in the formulation of protein biotherapeutics: structure and degradation pathways. *J Pharm Sci*. 2008;97(8):2924–35.
- Ha E, Wang W, Wang YJ. Peroxide formation in polysorbate 80 and protein stability. *J Pharm Sci*. 2002;91(10):2252–64.
- Kishore RSK, Kiese S, Fischer S, Pappenberger A, Grauschopf U, Mahler H-C. The degradation of Polysorbates 20 and 80 and its potential impact on the stability of biotherapeutics. *Pharm Res*. 2011;28(5):1194–210.
- Labrenz SR. Ester hydrolysis of Polysorbate 80 in mAb drug product: evidence in support of the hypothesized risk after the observation of visible particulate in mAb formulations. *J Pharm Sci*. 2014;103(8):2268–77.
- Tomlinson A, Demeule B, Lin B, Yadav S. Polysorbate 20 degradation in biopharmaceutical formulations: quantification of free fatty acids, characterization of particulates, and insights into the degradation mechanism. *Mol Pharm*. 2015;12(11):3805–15.
- Dixit N, Salamat-Miller N, Salinas PA, Taylor KD, Basu SK. Residual host cell protein promotes Polysorbate 20 degradation in a Sulfatase drug product leading to free fatty acid particles. *J Pharm Sci*. 2016;105(5):1657–66.
- Kishore RSK, Pappenberger A, Dauphin IB, Ross A, Buergi B, Staempfli A, et al. Degradation of polysorbates 20 and 80: studies on thermal autoxidation and hydrolysis. *J Pharm Sci*. 2011;100(2):721–31.
- Dwivedi M, Blech M, Presser I, Garidel P. Polysorbate degradation in biotherapeutic formulations: identification and discussion of current root causes. *Int J Pharm*. 2018;552(1):422–36.
- Doshi N, Demeule B, Yadav S. Understanding particle formation: solubility of free fatty acids as Polysorbate 20 degradation byproducts in therapeutic monoclonal antibody formulations. *Mol Pharm*. 2015;12(11):3792–804.
- Saggu M, Liu J, Patel A. Identification of subvisible particles in biopharmaceutical formulations using Raman spectroscopy provides insight into Polysorbate 20 degradation pathway. *Pharm Res*. 2015;32(9):2877–88.
- Chiu J, Valente KN, Levy NE, Min L, Lenhoff AM, Lee KH. Knockout of a difficult-to-remove CHO host cell protein, lipoprotein lipase, for improved polysorbate stability in monoclonal antibody formulations. *Biotechnol Bioeng*. 2017;114(5):1006–15.
- Katz JS, Nolin A, Yezer BA, Jordan S. Dynamic properties of novel excipient suggest mechanism for improved performance in liquid stabilization of protein biologics. *Mol Pharm*. 2019;16(1):282–91.
- Makwana S, Basu B, Makasana Y, Dharamsi A. Prefilled syringes: an innovation in parenteral packaging. *Int J Pharm Investig*. 2011;1(4):200–6.
- Sacha G, Rogers JA, Miller RL. Pre-filled syringes: a review of the history, manufacturing and challenges. *Pharm Dev Technol*. 2015;20(1):1–11.
- Sigma-Aldrich. Silicone Oil Safety Data Sheet (Aldrich - 378364). 2020.
- Doshi N, Fish R, Padilla K, Yadav S. Evaluation of super refined™ Polysorbate 20 with respect to Polysorbate degradation. *Journal of Pharmaceutical Sciences: Particle Formation and Protein Stability*; 2020.
- Hewitt D, Zhang T, Kao YH. Quantitation of polysorbate 20 in protein solutions using mixed-mode chromatography and evaporative light scattering detection. *J Chromatogr A*. 2008;1215(1–2):156–60.
- Hewitt D, Alvarez M, Robinson K, Ji J, Wang YJ, Kao YH, et al. Mixed-mode and reversed-phase liquid chromatography-tandem mass spectrometry methodologies to study composition and base hydrolysis of polysorbate 20 and 80. *J Chromatogr A*. 2011;1218(15):2138–45.
- McShan AC, Kei P, Ji JA, Kim DC, Wang YJ. Hydrolysis of Polysorbate 20 and 80 by a range of Carboxylester hydrolases. *PDA J Pharm Sci Technol*. 2016;70(4):332–45.
- Siska CC, Pierini CJ, Lau HR, Latypov RF, Fesinmeyer RM, Litowski JR. Free fatty acid particles in protein formulations, part 2: contribution of polysorbate raw material. *J Pharm Sci*. 2015;104(2):447–56.

25. Werk T, Volkin DB, Mahler HC. Effect of solution properties on the counting and sizing of subvisible particle standards as measured by light obscuration and digital imaging methods. *Eur J Pharm Sci.* 2014;53:95–108.
26. Barroso da Silva FL, Bogren D, Söderman O, Åkesson T, Jönsson B. Titration of fatty acids solubilized in cationic, nonionic, and anionic micelles. Theory and experiment. *The Journal of Physical Chemistry B.* 2002;106(13):3515–22.
27. Popović MR, Popović GV, Agbaba DD. The effects of anionic, cationic, and nonionic surfactants on Acid–Base Equilibria of ACE inhibitors. *J Chem Eng Data.* 2013;58(9):2567–73.
28. Tomlinson A, Zarraga IE, Demeule B. Characterization of Polysorbate Ester fractions and implications in protein drug product stability. *Mol Pharm.* 2020;17(7):2345–53.
29. Bravo B, Sánchez J, Cáceres A, Chávez G, Ysambert F, Márquez N, et al. Partitioning of fatty acids in oil/water systems analyzed by HPLC. *J Surfactant Deterg.* 2008;11(1):13–9.
30. Sangster J. Octanol-water partition coefficients of simple organic compounds. *J Phys Chem Ref Data.* 1989;18(3):1111–229.
31. LOGKOW databank [Internet]. Sangster Res. Lab. 1994.
32. Funke S, Matilainen J, Nalenz H, Bechtold-Peters K, Mahler HC, Friess W. Optimization of the bake-on siliconization of cartridges. Part I: optimization of the spray-on parameters. *Eur J Pharm Biopharm.* 2016;104:200–15.
33. Jones LS, Kaufmann A, Middaugh CR. Silicone oil induced aggregation of proteins. *J Pharm Sci.* 2005;94(4):918–27.
34. Lapelosa M, Patapoff TW, Zarraga IE. Molecular simulations of micellar aggregation of polysorbate 20 ester fractions and their interaction with N-phenyl-1-naphthylamine dye. *Biophys Chem.* 2016;213:17–24.
35. Nayem J, Zhang Z, Tomlinson A, Zarraga IE, Wagner NJ, Liu Y. Micellar morphology of Polysorbate 20 and 80 and their Ester fractions in solution via small-angle neutron scattering. *J Pharm Sci.* 2020;109(4):1498–508.

Publisher's Note Springer Nature remains neutral with regard to jurisdictional claims in published maps and institutional affiliations.